Current Science
CS 5 (4), 3817-3831 (2025)
Received 19 May 2025 | **Revised 16 June** 2025 | **Accepted 22 July**. 2025 | **Online Available 4 August** 2025
https://doi.org/ 10.52845/CS/2025-5-4-41

Current Science

Current Science

OPEN ACCESS

ISSN(O)2795-8639

Original Article

Downregulation of Programmed Cell Death Factor 4 Attenuated Post-Traumatic Stress Disorder-Like Behaviors in Mice by ERK/CREB Pathway

Rui Yue[1#], Ting Li[2#], Bing Gu[1#], Liwei Chai[3], Xinyu Zhou[1], Yijun Zhou[3], Zhen Wang[3], Haifeng Zhao[4*], Dexiang Liu[1]**

[1]Department of Medical Psychology and Ethics, School of Basic Medicine Sciences, Cheeloo College of Medicine, Shandong University, Jinan, Shandong, 250012, P.R. China

[2]Department of Psychiatry, Liaocheng People's Hospital, No. 67 Dongchang West Road, Dongchangfu District, Liaocheng, 252000, Shandong, P.R.China

[3]Department of Physiology, School of Basic Medical Sciences, Cheeloo College of Medicine, Shandong University, Jinan, Shandong, 250012, P.R. China

[4]Urology of Qilu hospital, Shandong University, Wenhuaxi road 107, Jinan,Shandong Province

#Bing Gu, Rui Yue and Ting Li Are Joint First Authors and Contributed Equally to this Work.

[*]Corresponding Author: Dr. Haifeng Zhao, Dr. Dexiang Liu

Abstract:
Post-traumatic stress disorder (PTSD) selectively develops in some individuals exposed to a traumatic event. However, the underlying mechanism of anxiety and depressive disorder in PTSD remains unclear. We found that mice receiving single-prolonged-stress (SPS) exhibited increased anxiety/depressive-like behaviors, memory deficits, and prolonged freezing time. Furthermore, cross-omics analyses of the Gene Expression Omnibus (GEO) database, including single-cell RNA sequencing and single-nucleus RNA sequencing from social defeat models or depressive models revealed the significantly upregulated transcripts of programmed cell death factor 4 (PDCD4) in multiple brain regions including hippocampus and lateral habenula. Here, we found that PDCD4 was significantly upregulated in the hippocampus of SPS mice. Further analyses revealed changes in the expressions of synaptic-associated proteins and BDNF, and in the phosphorylation of ERK/CREB paralleled the variation of PDCD4 levels in hippocampus of mice with PTSD-like behaviors. Finally, knockdown of PDCD4 significantly restored aberrant synaptic structures and alleviated PTSD-like behaviors via the ERK/CREB pathway in a SPS mouse model. Together, these results indicate that PDCD4 was involved in the synaptic plasticity and PTSD-like behaviors via the ERK/CREB pathway.

Keywords: Post-traumatic stress disorder, PDCD4, neuroplasticity, BDNF, ERK

1. Introduction

Post-traumatic stress disorder (PTSD), a debilitating psychiatric condition, manifests as maladaptive hyperreactivity to trauma-associated contextual cues and dysfunctional fear extinction processes. Core clinical features encompass intrusive re-experiencing (e.g., flashbacks), persistent hyperarousal (e.g., irrational fear), affective instability, comorbid anxiety-depressive symptomatology, and elevated suicidality risk(Bryant, 2019). Epidemiological data indicate that PTSD manifests in 10%–30% of individuals exposed to catastrophic events, with lifetime prevalence rates within this population ranging from 3% to 58%(Zafonte, 2017). Current therapeutic strategies for PTSD, including psychological interventions (e.g., cognitive behavioral therapy) and pharmacological approaches (e.g., antidepressant and antipsychotic

regimens), demonstrate efficacy in symptom mitigation. Nevertheless, the development of more targeted and potent treatment modalities remains imperative to address the unmet clinical needs and enhance functional outcomes in affected individuals.

Emerging evidence suggested that the pathophysiology of PTSD was intricately linked to hippocampal dysregulation, which manifests as impaired contextual discrimination of traumatic memories, maladaptive generalization of fear conditioning, and deficits in spatial working memory consolidation(Lopresto, Schipper, & Homberg, 2016). Neuroimaging investigations utilizing structural magnetic resonance imaging (MRI) had consistently revealed reduced hippocampal volume in PTSD patients, with pronounced volumetric deficits localized to the dentate gyrus (DG) and CA3 subfields, compared to both healthy controls and individuals diagnosed with social anxiety disorder(Irle et al., 2010; Kitayama, Vaccarino, Kutner, Weiss, & Bremner, 2005; Logue et al., 2018; Z. Wang et al., 2010). Accumulating evidence suggests chronic stress exposure may induce hippocampal damage through glucocorticoid-mediated mechanisms, primarily driven by sustained elevation of cortisol levels(Hoschl & Hajek, 2001; Swaab, Bao, & Lucassen, 2005). Consequently, structural and functional alterations in hippocampal neuronal circuits, particularly within the DG, may represent critical neurobiological substrates underlying the core symptomatology and behavioral manifestations of PTSD.

Programmed cell death 4 (PDCD4), a key regulator of apoptosis, plays a pivotal role in oncogenesis and inflammatory pathologies. Emerging evidence indicated that PDCD4 expression was significantly upregulated in the brains of individuals with depression. Furthermore, neuron-specific PDCD4 has been implicated in stress-induced depressive phenotypes, potentially through mechanisms involving the suppression of brain-derived neurotrophic factor (BDNF) signaling and the activation of pro-inflammatory cascades(Y. Jia et al., 2021; Li et al., 2021). Our findings further demonstrated that PDCD4 contributed to the enhanced vulnerability to depression following early-life stress exposure(Cheng et al., 2024). Nevertheless, the functional role and molecular mechanisms of PDCD4 in PTSD-like phenotypes remain poorly understood. In this study, we identified PDCD4 as a differentially expressed gene in multiple brain regions including hippocampus and lateral habenula (LHb) of social defeat models or depressive models through bioinformatics analysis of the Gene Expression Omnibus (GEO) database. Functional studies revealed that downregulation of PDCD4 ameliorated PTSD-like behaviors in a single prolonged stress (SPS) mouse model, potentially through modulation of the extracellular signal-regulated kinase (ERK)/ cAMP response element-binding protein (CREB) signaling pathway.

2. Materials and methods

2.1 Bioinformatics analysis

The Gene Expression Omnibus (GEO, http://www.ncbi.nlm.nih.gov/geo) database was used to collect single-cell RNA sequencing (scRNA-seq) and single-nucleus RNA sequencing (snRNA-seq) transcriptome data from social defeat models or depressive models. Control-Veh and repeated social defeat (RSD) mice-Veh groups were selected from the GSE275205 dataset for analysis. Naïve mice and chronic restraint stress (CRS) mice were selected from the GSE287308 dataset for analysis.

All scRNA-seq and snRNA-seq were processed using Seurat (v.5) in R (v.4.4.2) and each dataset was analyzed separately. In detail, each file was read and merged into a Seurat object. Cells with mitochondrial gene over-expression were filtered out (percentage. mt >5%). Normalize Data() was used to log-normalize the data and scale it to 10,000 transcripts per cell using Scale(). RunPCA() implemented Principal Component Analysis (PCA) for dimensionality reduction. Used ElbowPlot() to determine the first 12 principal components. Set the resolution of FindClusters() to 0.2. Used RunUMAP() and RunTSNE() for dimensionality reduction. And used the MouseRNAseqData dataset from the celldex package as a reference dataset and annotated the data using the SingleR package. This resulted in the identification of eight cell types: microglia, oligodendrocytes, neurons, endothelial cells, astrocytes, monocytes, epithelial cells, and erythrocytes. Used FindMarkers() to identify differentially expressed genes between groups, and filtered the genes with $p < 0.1$ and $|\text{logfc.threshold}| \geq 0.25$. Then, used the ggplot2

package to create a volcano plot. Finally, used the clusterProfiler package to perform Gene Ontology (GO) and Kyoto Encyclopedia of Genes and Genomes (KEGG) enrichment analysis on the differentially expressed genes.

2.2. Animals

All procedures involving animal care and experimentation were performed in compliance with the guidance of the Care and Use of Laboratory Animals from the National Institutes of Health and were approved by the Laboratory Animal Ethics Committee of Shandong University (Protocol No. ECSBMSSDU2022-2-83). Male C57BL/6J mice aged 7-8 weeks, obtained from Beijing Vital River Laboratory Animal Technology (Certification No. SCXK (Jing) 2021-0006), were housed under specific pathogen-free conditions at Shandong University animal facility. The mice were maintained in groups of five per cage under controlled environmental conditions, including a 12-h light/dark cycle and a constant temperature of 22 °C.

2.3. SPS procedure

Following the acclimatization phase, the mice were subjected to the SPS protocol, modified from an established methodology(Yu et al., 2024). The procedure consisted of three sequential phases: initial restraint in plexiglass tubes for 2 h, followed immediately by forced swimming in a cylindrical container (45 cm depth × 19 cm diameter) containing water maintained at ambient temperature for 20 min. After a 15-min recuperation interval, the mice were exposed to anhydrous diethyl ether until complete anesthesia was achieved, with this anesthetic procedure repeated twice. Subsequently, all subjects were transferred to clean cages with fresh bedding material and maintained without experimental intervention for a 7-day observation period.

2.4. Behavioral tests

Behavioral assessments were initiated 8 days following SPS exposure. The experimental procedures were performed in a controlled, low-noise environment with appropriate inter-test intervals. A standardized test sequence was implemented for all subjects, progressing from least to most stressful: (1) open field test, (2) elevated plus maze test, (3) conditioning fear test, (4) tail suspension test, and (5) forced swimming test. This hierarchical testing protocol was designed to reduce potential interference from preceding tests, as previously described(Li et al., 2022). All behavioral evaluations and data collection were conducted during the adult stage to ensure consistency, as stress response outcomes are known to exhibit age-dependent variability.

2.5 Stereotactic injections

The PDCD4 shRNA lentivirus (shPDCD4) and negative control shRNA (shNC) were commercially obtained from GenePharma. The mice were anesthetized using isoflurane inhalation and securely positioned in a stereotaxic apparatus. Stereotaxic coordinates for hippocampal targeting were determined relative to bregma (mediolateral: ±1.5 mm; anteroposterior: -2.00 mm; dorsoventral: -2.0 mm). Viral delivery was performed using a microinjection system, with lentiviral suspension ($1 \times 10^{\wedge 8}$ TU/mL) administered at a volume of 1.5 μL. The infusion rate was maintained at 0.5 μL per 3 min, followed by a 5-min post-injection interval.

2.6. Golgi staining

Neuronal morphology was analyzed using Golgi-Cox staining to evaluate dendritic spine density and morphological characteristics. Following the manufacturer's protocol, intact brains were immersed in the staining solution and maintained at room temperature under light-protected conditions for 14 days. Subsequently, the stained tissues were processed into 60-μm thick paraffin-embedded sections. The images were observed under a field of view of a microscope (Olympus, Tokyo, Japan) and analyzed quantitatively with ImageJ (NIH, Scion Corporation, Frederick, MD). Neuronal selection criteria included: (1) the presence of unobstructed terminal dendritic branches, (2) clear visualization of dendritic spines, and (3) a minimum dendritic length of 10 μm. Only cells meeting these criteria were included in the quantitative analysis of dendritic spine density and classification.

2.7 Statistical analysis

All data were expressed as mean ± standard deviation (SD). IBM SPSS statistics 26.0 software was used for analysis. If the data satisfied normal distribution, the data were analyzed with the Student's *t*-test (2 groups) or two-way analysis of variance (ANOVA) followed by the Bonferroni multiple comparisons test (details in figure legends). Correlation was measured using Pearson

correlation analysis. Statistical significance was indicated as follows: *$p < 0.05$, **$p < 0.01$, ***$p < 0.001$. GraphPad Prism 8.01 software was used for drawing.

The sample size was calculated in our pilot study to determine the smallest number of mice required to detect remarkable differences in the behavioral performance between Control and SPS group. Using a power analysis, 5 mice were allocated to each experimental group to detect behavioral performance.

3 Results

3.1 Bioinformatics analysis

We extracted a total of 9,371 cells derived from scRNA-seq datasets from the GSE275205. The omics data were derived from tissue in the hippocampus from RSD mice. This enhanced stress reactivity after RSD is clinically relevant and shares key elements with PTSD(Goodman et al., 2024).The dataset was further divided into 8 sub-datasets. After SingleR and reference to the previous literature, we integrated 8 major brain cell types (microglia, oligodendrocytes, endothelial cells, astrocytes, monocytes, epithelial cells, neuron and erythrocytes) (Figure 1A). We found that the majority of the cell types in hippocampus displayed transcriptomic alterations in RSD mice.

To determine specific genes that may be involved in RSD pathogenesis in each cell type and to further refine the sensitive cell types, we identified differentially expressed genes (DEGs) between control and RSD mice within each cell cluster (summary of DEGs in Table 1). At $p < 0.1$, the cell types that had hundreds of DEGs between control and RSD mice were ranked based on the number of DEGs over the number of expressed genes of that cell type, in the following order: Microglia (5.61% of expressed genes as DEGs) > endothelial (5.45%) > oligodendrocytes (1.82%) > epithelial cells (1.42%)> Neurons (0.51%) > astrocytes (0.16%) > monocytes (0.305%) (Table 1).

Table 1. DEGs of major cell types from brainstem cell populations of GSE275205.

Cell type	No. of Genes	No. of DEGs at |logfc.threshold| ≥ 0.25, *p* adj< 0.1	DEGs/Genes (%)
Microglia	3812	214	5.61
Endothelial cells	4803	262	5.45
Oligodendrocytes	5442	99	1.82
Epithelial cells	4661	66	1.42
Neurons	6419	33	0.51
Astrocytes	5022	8	0.16
Monocytes	4176	2	0.05

The volcano plot was performed to show the upregulated (1003) and downregulated (3122) transcriptional profiles related to RSD (Figure 1B) (p<0.05, logfc.threshold ≥ 0.25). We found that expression of *Pdcd4* mRNA was dramatically upregulated in RSD mice compared with control mice ($p < 0.001$, Figure 1C). Moreover, *Pdcd4* mRNA also showed significant differential expression in many cell types with mostly consistent directional changes across cell types (microglia, oligodendrocytes, endothelial cells, monocytes, epithelial cells, and neuron, Figure 1D). To discover the common transcription-level changes in depression and reveal the role of the functional pathways, we performed GO functional and KEGG pathway enrichment analyses of the intersecting DEGs and ranked enriched terms based on the number of intersecting genes involved. GO analysis showed that the DEGs were most significantly enriched in the biological activity of synaptic biological processes, such as postsynaptic membrane, postsynaptic density, asymmetric synapse (Figure 1E). KEGG analysis showed that intersecting DEGs were mainly associated with pathways of neurodegeneration-multiple diseases, PI3K-Akt signaling pathway, so on (Figure 1F).

Next, we accessed one dataset from the GEO database: snRNA-seq from the LHb of CRS and naïve mice (GSE287308). Four major brain cell types (neuron, oligodendrocytes, astrocytes and microglia) were found (Figure S1A). The volcano

plot was performed to show the upregulated (1003) and downregulated (2218) transcriptional profiles related to CRS (Figure S1B). We found that expression of *Pdcd4* mRNA was dramatically upregulated in CRS mice compared with control mice (p < 0.001, Figure S1C). We identified DEGs between control and RSD mice within each cell cluster (summary of DEGs in Table 2).

Table 2. DEGs of major cell types from brainstem cell populations of GSE287308.

Cell type	No. of Genes	No. of DEGs at |logfc.threshold| ≥ 0.25, *p_adj* < 0.1	DEGs/Genes (%)
Neurons	11082	2427	21.9
Oligodendrocytes	8142	626	7.69
Astrocytes	9622	681	7.08
Microglia	11445	2	0.02

By investigating intersecting DEGs in GSE275205 and GSE287308 by Venn diagram analysis, we identified 478 intersecting DEGs for further analyses (Figure 1G), of which 28 were upregulated (Figure 1H) and 282 was downregulated (Figure 1I). These intersecting DEGs included *Pdcd4*, which demonstrated *Pdcd4* significantly upregulated in the hippocampus and LHb in chronic stress group, compared to control group. Therefore, we chose PDCD4 as the research subject, which may be a potential important factor for SPS-induced PTSD-like behaviors.

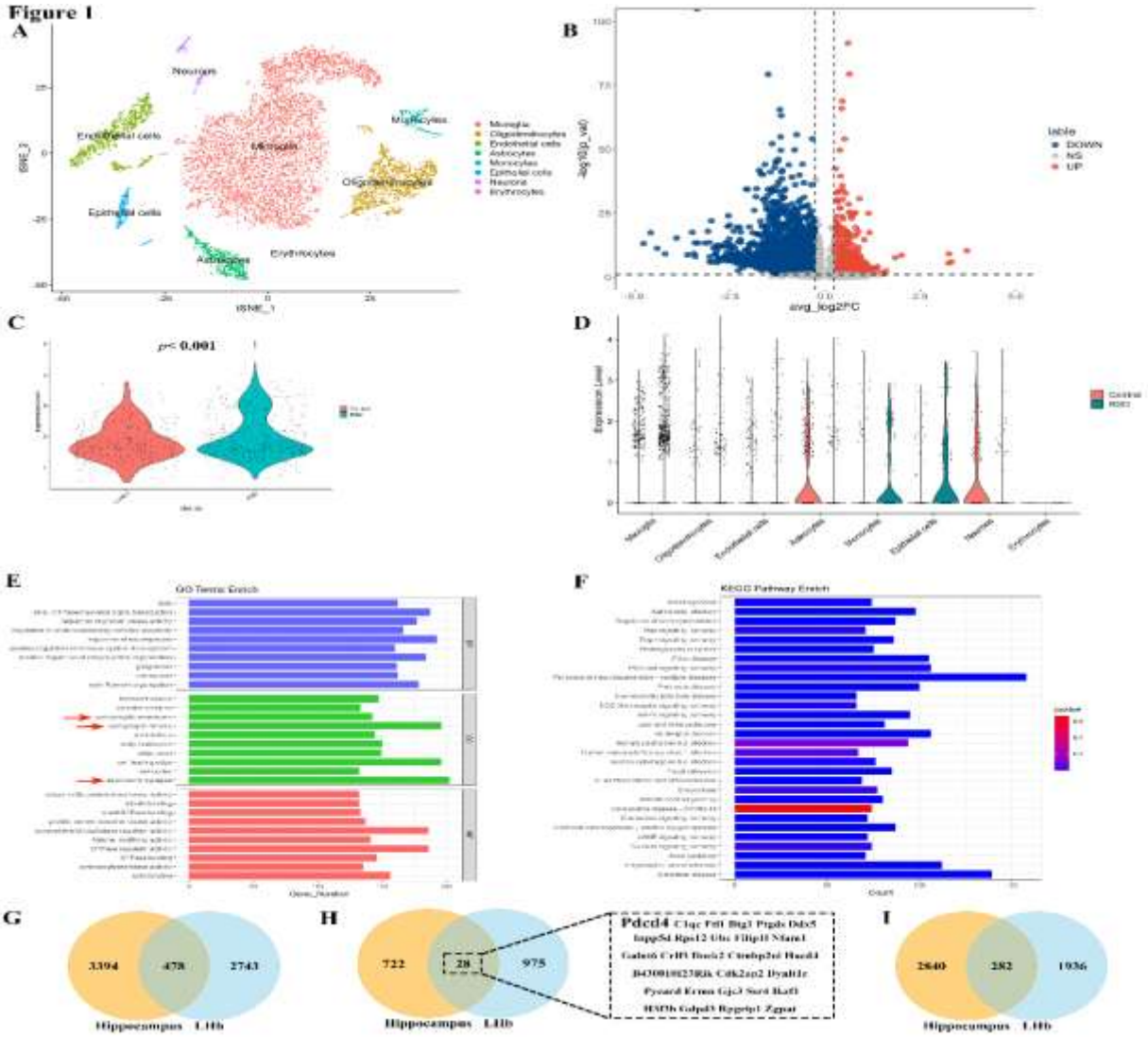

Figure 1 Major brainstem cell clusters and cell identities

(A) t-SNE plot from the GSE275205 visualizing clustering of single cells colored by cell types. (B) Volcano plot was performed to show the up-regulated and down-regulated transcriptional profiles related to RSD. (C) The *Pdcd4* mRNA was up-regulated in the hippocampus of RSD mice from the GSE275205. (D) The plot visualizing the expression distribution of *Pdcd4* mRNA in in many cell types. (E) GO analysis of DEGs of GSE275205. (F) KEGG analysis of DEGs of GSE275205. (G) The expression of intersected DEGs from GSE275205 and GSE287308. (H)The up- regulated expression of intersected DEGs from GSE275205 and GSE287308. (I)The down-regulated expression of intersected DEGs from GSE275205 and GSE287308. Results were presented as mean ± SD. ***$p < 0.001$ according to Student's *t*-test in C.

3.2 Temporal expression and localization of PDCD4 after SPS induction

In the OFT, mice in the SPS group spent significantly less time ($p < 0.001$, Figure 2B-D) in the central area compared to the control group. There was no statistically significant difference in the total traveling distance among the groups (Figure 2C). In the EPM, the decreased percentages of open arm entries ($p < 0.001$, Figure 2E,G) and the time spent ($p < 0.001$, Figure 2F,G) in the open arms were induced by the SPS. Our results showed that mice in the SPS group had significantly longer freezing times in both the contextual ($p < 0.001$, F Figure 2H) and cued (($p < 0.01$, Figure 2I) fear memory tests than those in the control group. Mice in SPS group showed an increase in immobility time during the TST ($p < 0.001$, Figure 2J) and FST ($p < 0.001$, Figure 2K). There were significant correlations between the central area time in OFT, open-arm entries and time in EPM, conditioned fear test, and immobility time in TST or FST within the same animals (Figure 2L), suggesting good coherence of these measures for the assessment of depressive-like phenotypes in mice.

All these data indicated that SPS model was successfully established and could be used for following assays. At last, we measured the protein levels of PDCD4 in hippocampal tissues of mice and found that the PDCD4 protein levels were increased in SPS group than that in control group ($p<0.01$, Figure 2M)

.

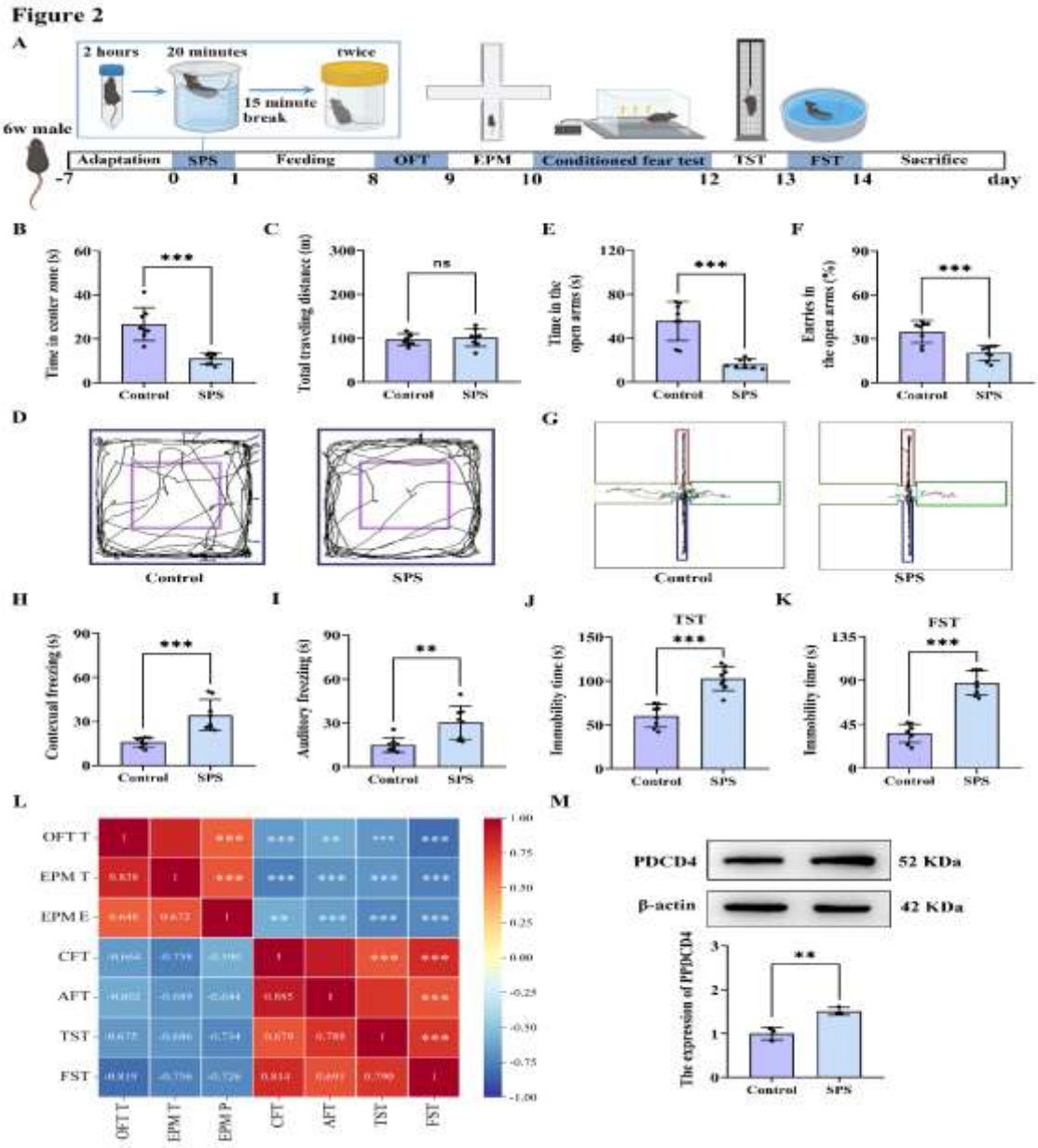

Figure 2 SPS mice were more likely to develop depression, anxiety-like symptoms, and social behavior disorders

(A) Experimental design flow chart. (B) The time spent in center zone in OFT. (C) The total traveling distance in OFT. (D) The travel pathway of OFT. (E) The duration of time spent in open arms in EPM test. (F) The entries in open arms in EPM test. (G) The trajectory of EPM test (H) The contextual freezing time. (I) The auditory freezing time. (J) The immobility time spent in TST. (K) The floating time spent in FST. (L) The correlations between the central area time in OFT (OFT T), open-arm entries (EPM E) and time in EPM (EPM T), conditioned fear test (CFT, contextual freezing time; AFT, auditory freezing time), and immobility time in TST or FST within the same animals. (M) Western blot detected expression of PDCD4 in the hippocampus. Results were presented as mean ± SD (N = 8 each group). *$p < 0.05$, **$p < 0.01$ and ***$p < 0.001$ according to Student's *t*-test in B, C, E, F, H, I, J, K, M. **$p < 0.01$ and ***$p < 0.001$ according to Pearson correlation analysis in L.

3.3 SPS-induced synaptic damage in the hippocampus, associating with reduced BDNF expression

Both basic and clinical studies have demonstrated that cortical and synaptic loss is strongly associated with depression. In this work, we tested whether SPS induced the changes in hippocampal synaptic plasticity of mice. Therefore, the dendritic complexity and spine density of CA1 and DG neurons as well as pyramidal cells were analyzed using Golgi staining. The reductions in

the number of intersections ($p < 0.01$, Figure 3A-B) and the longest length ($p < 0.001$, Figure 3A, C) of dendritic branches were pronounced in the SPS group compared with the control group. The number of intersections within 250 pixels represented in a line graph showed the same results ($p < 0.01$, Figure. 3D). Results showed that dendritic spine number ($p < 0.001$, Figure 3E, F) and density ($p < 0.001$, Figure 3E, G) were significantly reduced in SPS mice compared with controls.

PSD95 is the most important postsynaptic density (PSD) proteins involved in synaptic development and affects synaptic plasticity (H. Chen et al., 2022). The results showed that the expression of PSD95 was significantly decreased in mice exposed to SPS ($p < 0.01$, Figure 3H). The expression level of BDNF ($p < 0.05$, Figure 3I) was significantly lower in SPS mice than in the control group.

Figure 3

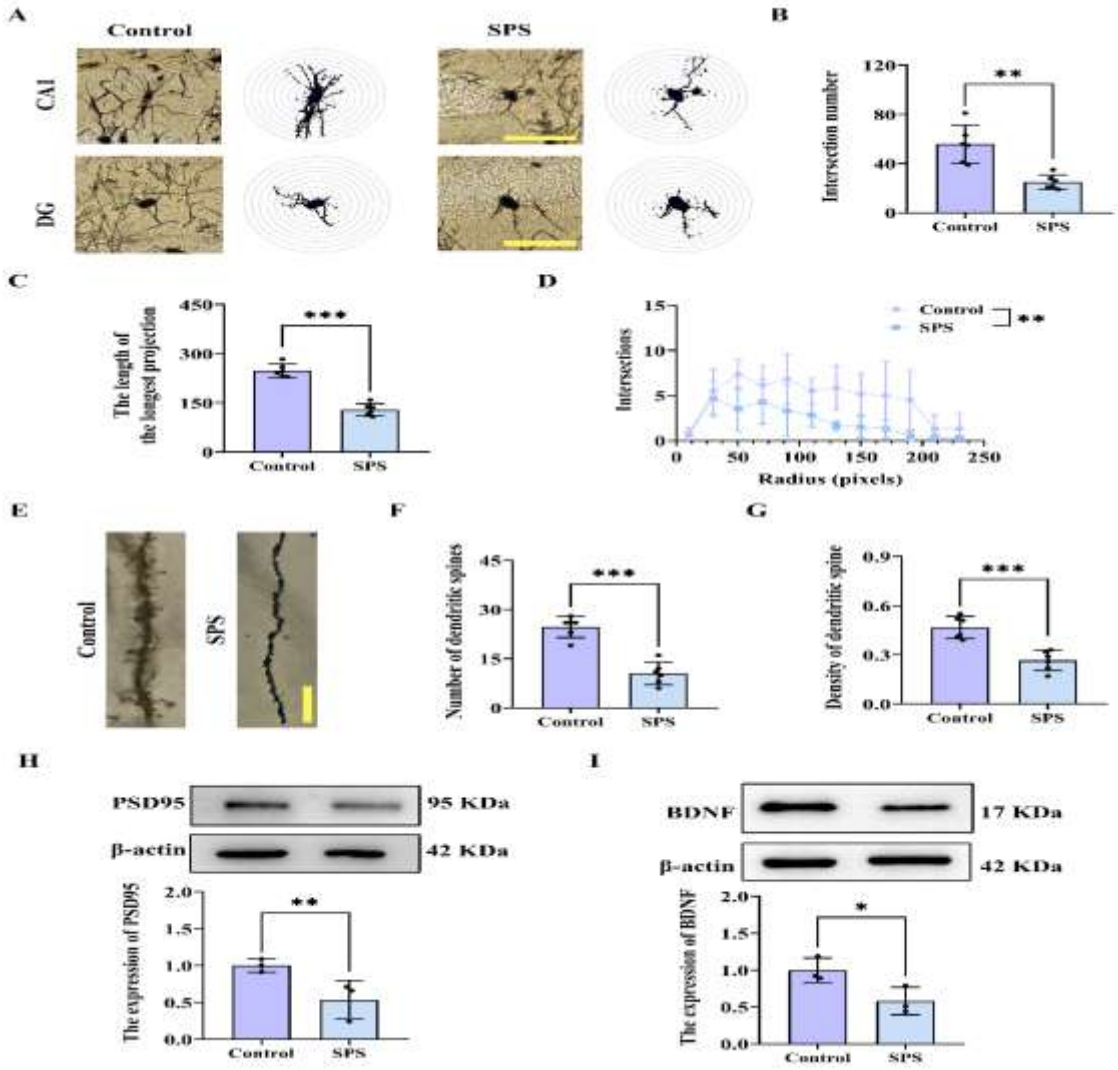

Figure 3 SPS-induced synaptic damage in the hippocampus, associating with reduced PSD95 and BDNF expression

(A) Representation of the Golgi staining of hippocampal adult neuron. (B) The number of intersections of dendritic branches from Golgi staining. (C) The longest length of dendritic branche. (D) The number of intersections within 250 pixels is represented in a line graph. (E) Golgi staining in the hippocampus. Scale bar = 10 µm. (F) Number of dendrite spines in the hippocampus. (G) The density of dendritic spine in the hippocampus. (H-I) Western blot detected expression of PSD95 and BDNF in the hippocampus. Results were presented as mean ± SD. *$p < 0.05$, **$p < 0.01$ and ***$p < 0.001$ according to Student's *t*-test in B, C, F, G, H, I and J. **$p < 0.01$ according to Two-way ANOVA test in D.

3.4 Knockout of PDCD4 expression mitigated PTSD-like behaviors of mice

To investigate the potential function of PDCD4 in PTSD-like behaviors, injection of lentivirus inhibiting PDCD4 expression was administered by intracerebroventricular injection (Figure 4A). Then, we validated the knockdown efficiency of PDCD4 lentivirus, and immunofluorescence results showed the infection effect of shPDCD4 in the hippocampus. Western blot analysis revealed a significant decrement in the expression of PDCD4 within the hippocampus of the shPDCD4 group compared to the shNC control group ($p < 0.05$, Figure 4B).

Mice in shPDCD4 group demonstrated a significant increase in the time in the center zone in OFT ($p < 0.05$, Figure 4C, E), the time of entering the open arm ($p < 0.01$, Fig. 4F, H) and the number of entering the open arm ($p < 0.01$, Figure 4G,H) in EPM. There was no statistically significant difference in the total traveling distance among the groups (Figure 4D). Mice in the shPDCD4 group had significantly less freezing times in both the contextual ($p < 0.01$, Fig. 4I) and cued ($p < 0.05$, Figure 4J) fear memory tests than those in the control group. Meanwhile, shPDCD4 group inhibited the increase in immobility time during the TST ($p < 0.05$, Figure 4K) and FST ($p < 0.01$, Figure 4L). These results suggest that knockout of PDCD4 expression alleviates the depressive behavior induced by SPS.

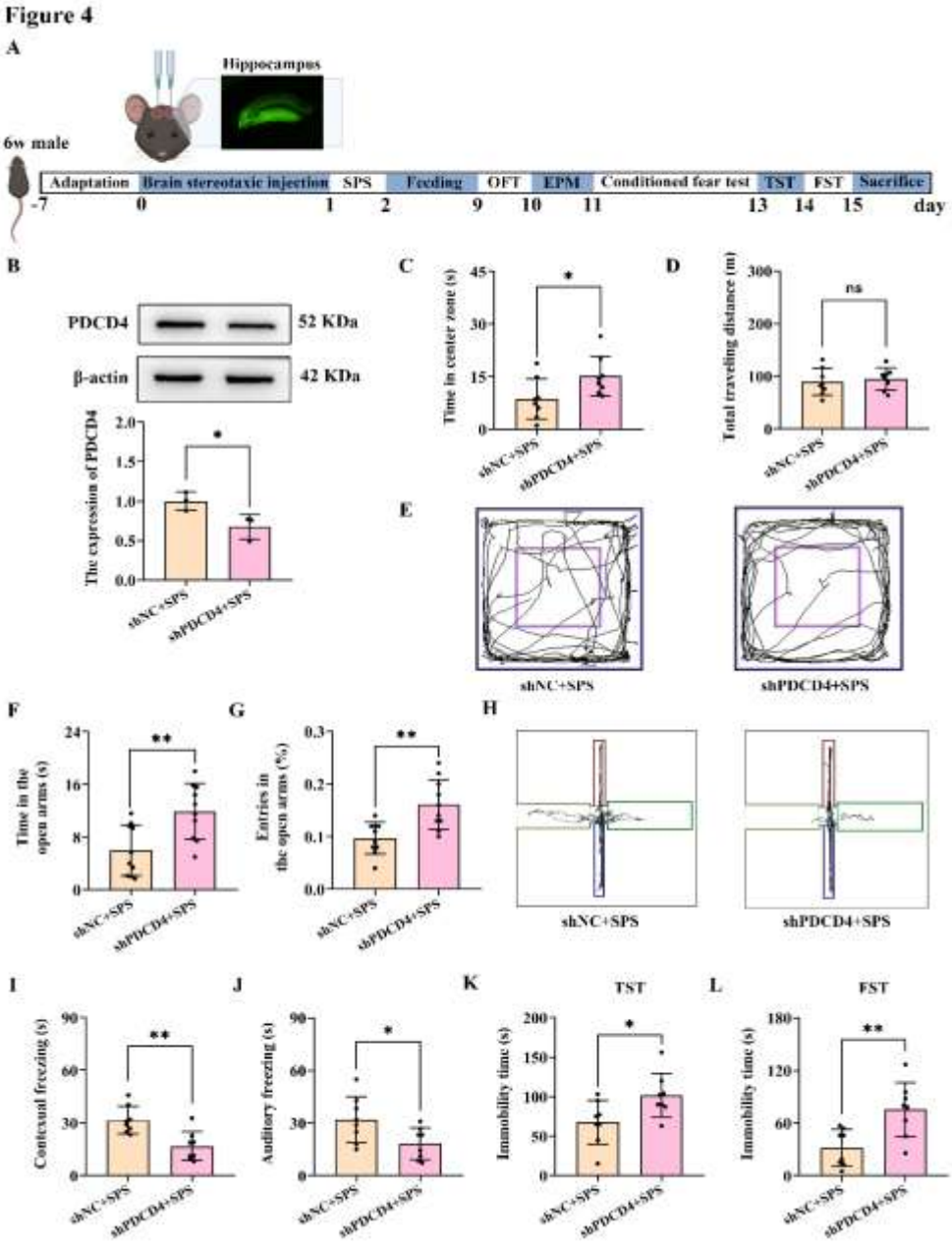

Figure 4 Knockout of PDCD4 expression mitigated PTSD-like behaviors of mice

(A) Experimental design flow chart. (B) Western blot detected expression of PDCD4 in the hippocampus. (C) The time spent in center zone in OFT. (D) The total traveling distance in OFT. (E) The travel pathway of OFT. (F) The duration of time spent in open arms in EPM test. (G) The entries in open arms in EPM test. (H) The trajectory of EPM test. (I) The contextual freezing time. (J) The auditory freezing time. (K) The immobility time spent in TST. (L) The floating time spent in FST. Results were presented as mean ± SD (N = 10 each group). *$p < 0.05$, **$p < 0.01$ and ***$p < 0.001$ according to Student's *t*-test.

3.5 Knockout of PDCD4 prevented SPS-induced synaptic damage in the hippocampus and normalized BDNF levels

The number of intersections ($p < 0.001$, Figure 5A, B) and the longest length ($p < 0.01$, Figure 5A, C) of dendritic branches of hippocampus were increased in shPDCD4 group. The number of intersections within 250 pixels represented in a line graph showed the same result ($p < 0.01$, Figure 5D). The dendritic spine number ($p < 0.01$, Figure 5E, F) and density ($p < 0.01$, Figure 5E, G) were significantly increased in shPDCD4 mice compared with shNC. The expression of PSD95 ($p < 0.05$, Figure 5H) and BDNF ($p < 0.05$, Figure5I) were significantly increased in shPDCD4 mice ($p < 0.01$, Figure 5H, I).

Figure 5

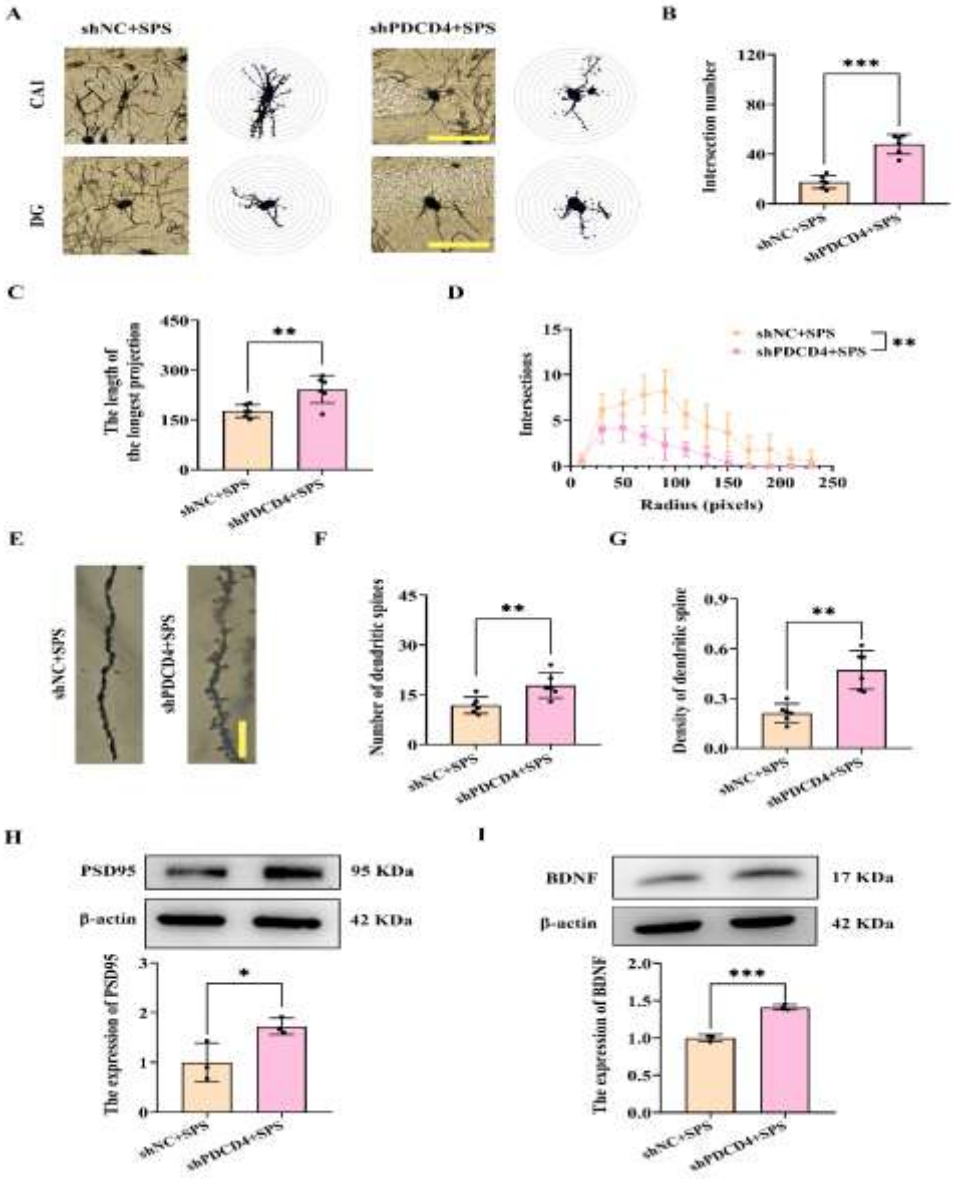

Figure 5 Knockout of PDCD4 prevented SPS-induced synaptic damage in the hippocampus

(A) Representation of the Golgi staining of hippocampal adult neuron. (B) The number of intersections of dendritic branches from Golgi staining. (C) The longest length of dendritic branche. (D) The number of intersections within 250 pixels is represented in a line graph. (E) Golgi staining in the hippocampus. Scale bar = 10 µm. (F) Number of dendrite spines in the hippocampus. (G) The density of dendritic spine in the hippocampus. (H-I) Western blot detected expression of PSD95 and BDNF in the hippocampus. Results were presented as mean ± SD. *$p < 0.05$, **$p < 0.01$ and ***$p < 0.001$ according to Student's *t*-test in B, C, F, G, H, I and J. **$p < 0.01$ according to Two-way ANOVA test in D.

3.6 Knockout of PDCD4 upregulates the ERK/CREB signaling pathway in the hippocampus of SPS mice

The ERK1/2 signaling can be activated in response to diverse extracellular stimuli, and is involved in neuronal survival, growth, development and differentiation, subsequently affecting PTSD development. SPS significantly decreased the expression of the pERK/ERK ($p < 0.05$, Figure 6A) in the hippocampus compared to control. There were significant correlations between pERK/ERK and immobility time in TST (Figure 6B). The expression of pERK/ERK was significantly increased in shPDCD4 mice ($p < 0.05$, Figure 6C).

CREB plays a key role in promoting cell survival, precursor proliferation, neurite outgrowth, and neuronal differentiation in the nervous system, which can be activated with phosphorylation at Ser133 through ERK1/2. SPS significantly decreased the expression of the pCREB/CREB ($p < 0.05$, Figure 6D) in the hippocampus compared to control. There were significant correlations between pCREB/CREB and immobility time in TST (Figure 6E). The expression of pCREB/CREB was significantly increased in shPDCD4 mice ($p < 0.5$, Figure 6F). Upon SPS exposure, PDCD4 is involved in neuronal plasticity by decreasing levels of BDNF, p-ERK and p-CREB within hippocampus.

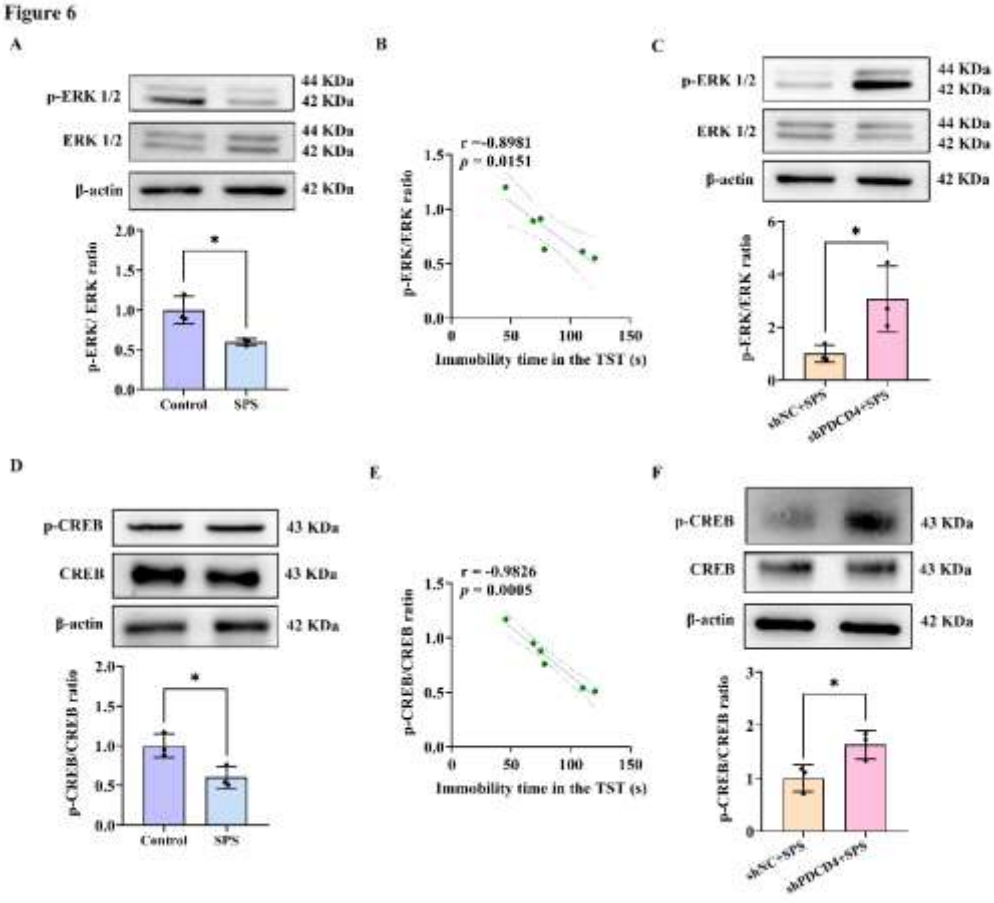

Figure 6 Knockout of PDCD4 reversed SPS induced inactivation of the ERK and CREB in the

hippocampus

Representative blots of molecular expression in the hippocampus. (A)The relative quantitative ratio of p-ERK/ERK in the hippocampus from all groups. (B) The correlations between p-ERK/ERK and immobility time in TST. (C) The relative quantitative ratio of p-ERK/ERK in the hippocampus from all groups. (D) The relative quantitative ratio of p-CERB/CERB in the hippocampus from all groups. (E) The correlations between p-CERB/CERB and immobility time in TST. (F) The relative quantitative ratio of p-CERB/CERB in the hippocampus from all groups. Results were presented as mean ± SD. *$p < 0.05$ according to Student's *t*-test in A, C, D, F. Pearson correlation analysis in B and E.

4 Discussion

The cross-omics analyses of GEO database, including scRNA-seq and snRNA-seq from social defeat model or depressive model revealed the significantly upregulated transcripts of PDCD4 in hippocampus. Meanwhile, we found that PDCD4 was significantly upregulated in the hippocampus of SPS mice. Further *in vivo and in vitro* analyses revealed that the changes in the expressions of PSD95 and BDNF and in the phosphorylation of ERK/CREB paralleled the variation of PDCD4 levels in the hippocampus in mice with PTSD-like behaviors. Suppression of PDCD4 significantly alleviated SPS-induced PTSD-like behavior by regulating the ERK/CREB pathway.

As an apoptotic regulator, the role of PDCD4 in the brain has been widely concerned. PDCD4 expression was increased in brain following LPS treatment in mice, association with microglial activation and neuronal apoptosis(Li et al., 2024; Sachdev, 1986). The changed PDCD4 expression has been found in brain tissue of cerebral ischemia and Parkinson's disease animal model, involved in neural cell apoptosis and mitochondrial injury(Li et al., 2023; Zhang, Lu, Guo, & Wang, 2025). The changed PDCD4 expression has also been observed in spinal cord injury animal model, indicating its involvement in nerve damage and repair(J. Wang, Zhao, Tang, Li, & Chen, 2021). Chronic restraint stress up-regulated PDCD4 expression in hippocampus, which impairs synaptic plasticity through suppression of BDNF mRNA translation and consequently results in the depression-like behaviors in mice(Li et al., 2021). Targeted delivery of PDCD4 specific siRNA protected mice from chronic restraint stress-induced depressive behavior, associating with up-regulating the level of BDNF and down-regulating IL-6 and IL-1β expression(Y. Jia et al., 2021). We also found that PDCD4 is involved the early life stress-induced susceptibility to depression(Cheng et al., 2024). Here, cross-omics analyses showed that PDCD4 was highly expressed in the hippocampus of social defeat model or depressive model. We also found the increased PDCD4 in the hippocampus of SPS mice, and suppression of PDCD4 significantly alleviated PTSD-like phenotype in SPS mice.

Synaptic plasticity, a fundamental property of neural circuits, encompasses dynamic alterations in synaptic number, structural morphology, and functional activity in response to diverse physiological and pathological stimuli(Tartt, Mariani, Hen, Mann, & Boldrini, 2022). Dysregulated synaptic plasticity represents a critical neurobiological mechanism contributing to the pathogenesis of PTSD symptomatology (Izquierdo, Furini, & Myskiw, 2016). Numerous preclinical investigations have explored the efficacy of therapeutic interventions for PTSD by examining their impact on synaptic plasticity dynamics (Yu et al., 2024). For instance, sevoflurane administration has been demonstrated to mitigate apoptotic processes and enhance hippocampal synaptic plasticity in rodent models of PTSD(Gu et al., 2023). In the present study, we observed a significant reduction in dendritic complexity and spine density within CA1 and DG neurons compared to control animals. Concurrently, diminished expression levels of PSD95, synaptotagmin-1 (Syt1), and BDNF in the hippocampus further corroborated the impairment of synaptic plasticity. Notably, PDCD4 knockdown reversed these synaptic abnormalities, restoring both structural integrity and synaptic protein expression in the hippocampus of SPS-exposed mice. These findings suggested that PDCD4 might contribute to PTSD-like phenotypes through modulation of synaptic plasticity mechanisms.

Our results suggest that PDCD4 affects BDNF/ PSD95 and ERK/CREB signaling in the

hippocampus of SPS mice. The current study revealed that the increase of PDCD4 expression accompanied the decrease of synaptic plasticity-related molecules, BDNF and PSD95, and the downregulation of the ERK/CREB pathway in mouse PTSD models. Additionally, the available data show that ERK plays a pivotal role in various neuropsychiatric disorders including depression (Si et al., 2023; L. Zhuang et al., 2024). Knockdown of PDCD4 significantly inhibited the phosphorylation of ERK and thus attenuated the LPS-induced microglial inflammatory activation (Q. Chen et al., 2022). MiR-21 can promote the proliferation, migration, and inhibit the apoptosis of human melanoma A375 cells by inhibiting SPRY1, PDCD4, and PTEN via ERK/NF-κB signaling pathway(Pruchno & Resch, 1989). Microglial ERK/CREB/BDNF signaling in the mPFC is involved in depression-like behaviors of chronic social defeat stress susceptible mice(Yao et al., 2022). HnRNPK in the hippocampal neurons is involved in stress-induced depression-like behavior via ERK/BDNF pathway in mice(L. P. Zhuang et al., 2023). Baicalin has antidepressant effects in chronic unpredictable mild stress-induced mice, associated with activation of the BDNF/ERK/CREB signaling pathway in the hippocampus(Z. Jia et al., 2021). Here, we found that the increased of phosphorylation of ERK and CREB, and the expressions of BDNF and PSD95 in the hippocampus of SPS mice can be attenuated by knocked down of PDCD4. Therefore, we infer that PDCD4 is involved in the development of PTSD-like phenotype through ERK/CREB-mediated the expression of BDNF and PSD95 in mice, of course, which requires further *in vivo* studies to confirm.

There are several limitations in our study. First, we only observed the neurobiological changes in the hippocampus region of mice. In fact, other brain regions (such as prefrontal cortex and nucleus accumbens) have been proven to be related to the process of fear memories(Ressler et al., 2022). Further research on the neurobiological changes induced by SPS in other brain regions, as well as the role of PDCD4 in these changes, is a key focus that we need to pay attention to. Second, we prioritized the role of PDCD4 effect on synaptic plasticity, but did not fully investigate the effects of PDCD4 on other factors that contribute to the pathogenesis of PTSD, such as neuroinflammation or epigenetic changes (Lv et al., 2023). A comprehensive understanding of the impact of PDCD4 on these factors can support its potential as a therapeutic agent. Third, we only studied the effect of organizational structural changes on synaptic transmission, and further electrophysiological experiments are needed to investigate the impact on synaptic function. Finally, we only focused on ERK/CREB/BDNF signaling pathway, while other signaling pathway required more exploration.

In conclusion, from cross-omics analyses and animal experiment, it has been demonstrated that PDCD4 involved in the pathogenesis of PTSD-like phenotype via the ERK/CREB/BDNF signaling pathway. These findings signify that modulating PDCD4 expression may serve as a promising candidate for the treatment of PTSD.

Funding

Research funding support for this work was from the National Natural Science Foundation of China (No. 82271327 and 82072535) to Dr. Zhen Wang and Natural Foundation of Shandong Provine (No. ZR2024MH038) to Dr. Zhen Wang.

Acknowledgments

We thank Translational Medicine Core Facility of Shandong University for consultation and instrument availability that supported this work.

Data Availability

The data underlying this article are available in the article and in its online supplementary material.

Competing Interests

The authors have no relevant financial or non-financial interests to disclose.

Author Contributions

DXL and HFZ designed the study and reviewed and revised the manuscript. RY and BG performed major experiments. TL performed GEO data analysis and analyzed the data and final revision of the manuscript. LWC performed GEO data analysis. XYZ and YJZ performed the behavioral experiment. ZW Resources, Funding acquisition. All authors read and approved the final manuscript. All authors contributed to review and editing of the manuscript.

Reference

1. Bryant, R. A. (2019). Post-traumatic stress dis order: a state-of-the-art review of evidence an d challenges. *World Psychiatry, 18*(3), 259-26 9. doi:10.1002/wps.20656
2. Chen, H., Qiao, D., Wang, C., Zhang, B., Wan g, Z., Tang, L., . . . Cui, H. (2022). Fragile X Mental Retardation Protein Mediates the Effec ts of Androgen on Hippocampal PSD95 Expre ssion and Dendritic Spines Density/Morpholo gy and Autism-Like Behaviors Through miR-1 25a. *Frontiers In Cellular Neuroscience, 16*, 8 72347. doi:10.3389/fncel.2022.872347
3. Chen, Q., Lu, H., Duan, C., Zhu, X., Zhang, Y., Li, M., & Zhang, D. (2022). PDCD4 Simul taneously Promotes Microglia Activation via P DCD4-MAPK-NF-kappaB Positive Loop and Facilitates Neuron Apoptosis During Neuroinf lammation. *Inflammation, 45*(1), 234-252. doi: 10.1007/s10753-021-01541-9
4. Cheng, J., Yuan, L., Yu, S., Gu, B., Luo, Q., W ang, X., . . . Ho, C. S. H. (2024). Programmed cell death factor 4-mediated hippocampal syna ptic plasticity is involved in early life stress an d susceptibility to depression. *Behav Brain Re s, 468*, 115028. doi:10.1016/j.bbr.2024.115028
5. Goodman, E. J., Biltz, R. G., Packer, J. M., Di Sabato, D. J., Swanson, S. P., Oliver, B., . . . G odbout, J. P. (2024). Enhanced fear memory af ter social defeat in mice is dependent on interl eukin-1 receptor signaling in glutamatergic ne urons. *Mol Psychiatry, 29*(8), 2321-2334. doi: 10.1038/s41380-024-02456-1
6. Gu, T., Xu, C., Meng, X., Gao, D., Jiang, G., Y in, A., . . . Zhang, L. (2023). Sevoflurane Prec onditioning Alleviates Posttraumatic Stress Di sorder-Induced Apoptosis in the Hippocampus via the EZH2-Regulated Akt/mTOR Axis and Improves Synaptic Plasticity. *J Mol Neurosci, 73*(4-5), 225-236. doi:10.1007/s12031-023-02 114-1
7. Hoschl, C., & Hajek, T. (2001). Hippocampal damage mediated by corticosteroids--a neurop sychiatric research challenge. *Eur Arch Psychi atry Clin Neurosci, 251 Suppl 2*, II81-88. doi:1 0.1007/BF03035134
8. Irle, E., Ruhleder, M., Lange, C., Seidler-Bran dler, U., Salzer, S., Dechent, P., . . . Leichsenri ng, F. (2010). Reduced amygdalar and hippoca mpal size in adults with generalized social pho bia. *J Psychiatry Neurosci, 35*(2), 126-131. do i:10.1503/jpn.090041
9. Izquierdo, I., Furini, C. R., & Myskiw, J. C. (2 016). Fear Memory. *Physiol Rev, 96*(2), 695-7 50. doi:10.1152/physrev.00018.2015
10. Jia, Y., Zhuang, X., Zhang, Y., Zhao, M., Che n, N., Li, W., . . . Zhang, L. (2021). The brain t argeted delivery of programmed cell death 4 s pecific siRNA protects mice from CRS-induce d depressive behavior. *Cell Death Dis, 12*(11), 1077. doi:10.1038/s41419-021-04361-9
11. Jia, Z., Yang, J., Cao, Z., Zhao, J., Zhang, J., L u, Y., . . . Pei, L. (2021). Baicalin ameliorates c hronic unpredictable mild stress-induced depre ssion through the BDNF/ERK/CREB signalin g pathway. *Behav Brain Res, 414*, 113463. do i:10.1016/j.bbr.2021.113463
12. Kitayama, N., Vaccarino, V., Kutner, M., Weis s, P., & Bremner, J. D. (2005). Magnetic reson ance imaging (MRI) measurement of hippoca mpal volume in posttraumatic stress disorder: a meta-analysis. *J Affect Disord, 88*(1), 79-86. doi:10.1016/j.jad.2005.05.014
13. Li, Y., Du, Y., Wang, C., Lu, G., Sun, H., Kon g, Y., . . . Sun, L. (2022). (2R,6R)-hydroxynor ketamine acts through GluA1-induced synapti c plasticity to alleviate PTSD-like effects in rat models. *Neurobiol Stress, 21*, 100503. doi:10. 1016/j.ynstr.2022.100503
14. Li, Y., Jia, Y., Wang, D., Zhuang, X., Li, Y., G uo, C., . . . Zhang, L. (2021). Programmed cell death 4 as an endogenous suppressor of BDNF translation is involved in stress-induced depres sion. *Mol Psychiatry, 26*(6), 2316-2333. doi:1 0.1038/s41380-020-0692-x
15. Li, Y., Pang, J., Wang, J., Dai, G., Bo, Q., Wan g, X., & Wang, W. (2023). Knockdown of PD CD4 ameliorates neural cell apoptosis and mit ochondrial injury through activating the PI3K/ AKT/mTOR signal in Parkinson's disease. *J C hem Neuroanat, 129*, 102239. doi:10.1016/j.jc hemneu.2023.102239
16. Li, Y., Zhan, B., Zhuang, X., Zhao, M., Chen, X., Wang, Q., . . . Zhang, L. (2024). Microglial Pdcd4 deficiency mitigates neuroinflammation -associated depression via facilitating Daxx m ediated PPARgamma/IL-10 signaling. *J Neuro inflammation, 21*(1), 143. doi:10.1186/s12974-024-03142-3
17. Logue, M. W., van Rooij, S. J. H., Dennis, E. L., Davis, S. L., Hayes, J. P., Stevens, J. S., . . . Morey, R. A. (2018). Smaller Hippocampal Vo lume in Posttraumatic Stress Disorder: A Multi site ENIGMA-PGC Study: Subcortical Volum

etry Results From Posttraumatic Stress Disorder Consortia. *Biol Psychiatry, 83*(3), 244-253. doi:10.1016/j.biopsych.2017.09.006

18. Lopresto, D., Schipper, P., & Homberg, J. R. (2016). Neural circuits and mechanisms involved in fear generalization: Implications for the pathophysiology and treatment of posttraumatic stress disorder. *Neurosci Biobehav Rev, 60*, 31-42. doi:10.1016/j.neubiorev.2015.10.009
19. Lv, T., Wang, M., Zheng, H. S., Mao, J. D., Yang, F., Yang, L., . . . Wu, Y. M. (2023). Electroacupuncture alleviates PTSD-like behaviors by modulating hippocampal synaptic plasticity via Wnt/beta-catenin signaling pathway. *Brain Res Bull, 202*, 110734. doi:10.1016/j.brainresbull.2023.110734
20. Pruchno, R. A., & Resch, N. L. (1989). Husbands and wives as caregivers: antecedents of depression and burden. *Gerontologist, 29*(2), 159-165. doi:10.1093/geront/29.2.159
21. Ressler, K. J., Berretta, S., Bolshakov, V. Y., Rosso, I. M., Meloni, E. G., Rauch, S. L., & Carlezon, W. A., Jr. (2022). Post-traumatic stress disorder: clinical and translational neuroscience from cells to circuits. *Nat Rev Neurol, 18*(5), 273-288. doi:10.1038/s41582-022-00635-8
22. Sachdev, P. S. (1986). Doctors' strike--an ethical justification. *N Z Med J, 99*(803), 412-414. Retrieved from https://www.ncbi.nlm.nih.gov/pubmed/3461354
23. Si, L., Xiao, L., Xie, Y., Xu, H., Yuan, G., Xu, W., & Wang, G. (2023). Social isolation after chronic unpredictable mild stress perpetuates depressive-like behaviors, memory deficits and social withdrawal via inhibiting ERK/KEAP1/NRF2 signaling. *J Affect Disord, 324*, 576-588. doi:10.1016/j.jad.2022.12.092
24. Swaab, D. F., Bao, A. M., & Lucassen, P. J. (2005). The stress system in the human brain in depression and neurodegeneration. *Ageing Res Rev, 4*(2), 141-194. doi:10.1016/j.arr.2005.03.003
25. Tartt, A. N., Mariani, M. B., Hen, R., Mann, J. J., & Boldrini, M. (2022). Dysregulation of adult hippocampal neuroplasticity in major depression: pathogenesis and therapeutic implications. *Mol Psychiatry, 27*(6), 2689-2699. doi:10.1038/s41380-022-01520-y
26. Wang, J., Zhao, Y., Tang, Y., Li, F., & Chen, X. (2021). The role of lncRNA-MEG/miR-21-5p/PDCD4 axis in spinal cord injury. *Am J Transl Res, 13*(2), 646-658. Retrieved from https://www.ncbi.nlm.nih.gov/pubmed/33594315
27. Wang, Z., Neylan, T. C., Mueller, S. G., Lenoci, M., Truran, D., Marmar, C. R., . . . Schuff, N. (2010). Magnetic resonance imaging of hippocampal subfields in posttraumatic stress disorder. *Arch Gen Psychiatry, 67*(3), 296-303. doi:10.1001/archgenpsychiatry.2009.205
28. Yao, W., Cao, Q., Luo, S., He, L., Yang, C., Chen, J., . . . Zhang, J. C. (2022). Microglial ERK-NRBP1-CREB-BDNF signaling in sustained antidepressant actions of (R)-ketamine. *Mol Psychiatry, 27*(3), 1618-1629. doi:10.1038/s41380-021-01377-7
29. Yu, S., Zhang, W., Wang, X., Luo, Q., Gu, B., Zhao, Y., . . . Wang, Z. (2024). H(2)S improves hippocampal synaptic plasticity in SPS rats via PI3K/AKT signaling pathway. *Brain Res, 1845*, 149286. doi:10.1016/j.brainres.2024.149286
30. Zafonte, R. D. (2017). Traumatic brain injury: an enduring challenge. *Lancet Neurol, 16*(10), 766-768. doi:10.1016/S1474-4422(17)30300-9
31. Zhang, Y., Lu, H., Guo, T., & Wang, J. (2025). SMAD1 Regulates the Hippocampal Neuronal Death and Ferroptosis via Affecting the Transcription of PDCD4 in Cerebral Ischemia. *Mol Neurobiol, 62*(2), 1960-1970. doi:10.1007/s12035-024-04379-y
32. Zhuang, L., Gao, W., Chen, Y., Fang, W., Lo, H., Dai, X., . . . Zhang, J. (2024). LHPP in Glutamatergic Neurons of the Ventral Hippocampus Mediates Depression-like Behavior by Dephosphorylating CaMKIIalpha and ERK. *Biol Psychiatry, 95*(5), 389-402. doi:10.1016/j.biopsych.2023.08.026
33. Zhuang, L. P., Gao, W. J., Fang, L. L., Zeng, G. R., Ye, Q. Y., Dai, X. M., . . . Chen, X. C. (2023). HnRNPK is involved in stress-induced depression-like behavior via ERK-BDNF pathway in mice. *Neurochem Int, 169*, 105589. doi:10.1016/j.neuint.2023.105589